THE JOURNAL OF BIOLOGICAL CHEMISTRY VOL. 287, NO. 40, pp. 33412–33423, September 28, 2012
© 2012 by The American Society for Biochemistry and Molecular Biology, Inc. Published in the U.S.A.

Replication Fork Stalling and Checkpoint Activation by a *PKD1* Locus Mirror Repeat Polypurine-Polypyrimidine (Pu-Py) Tract*

Received for publication, July 18, 2012 Published, JBC Papers in Press, August 6, 2012, DOI 10.1074/jbc.M112.402503

Guoqi Liu[‡1], **Sheré Myers**[‡], **Xiaomi Chen**[‡], **John J. Bissler**[§], **Richard R. Sinden**[¶2], **and Michael Leffak**[‡3]

From the [‡]*Department of Biochemistry and Molecular Biology, Boonshoft School of Medicine, Wright State University, Dayton, Ohio 45435, the* [§]*Division of Nephrology and Hypertension, Cincinnati Children's Hospital Medical Center, Cincinnati, Ohio 45229, and the* [¶]*Department of Biological Sciences, Florida Institute of Technology, Melbourne, Florida 32901*

Background: Repeated sequence non-B DNA structures impede replication forks and produce replication stress.
Results: A *PKD1* polypurine-polypyrimidine mirror repeat sequence stalls replication forks in an orientation-dependent manner.
Conclusion: Non-B DNA structure formation of the Pu-rich lagging strand template leads to checkpoint activation.
Significance: Deciphering how non-B DNA structures provoke replication stress, checkpoint activation, and adaptation is important for understanding genome instability diseases.

DNA sequences prone to forming noncanonical structures (hairpins, triplexes, G-quadruplexes) cause DNA replication fork stalling, activate DNA damage responses, and represent hotspots of genomic instability associated with human disease. The 88-bp asymmetric polypurine-polypyrimidine (Pu-Py) mirror repeat tract from the human polycystic kidney disease (*PKD1*) intron 21 forms non-B DNA secondary structures *in vitro*. We show that the *PKD1* mirror repeat also causes orientation-dependent fork stalling during replication *in vitro* and *in vivo*. When integrated alongside the c-*myc* replicator at an ectopic chromosomal site in the HeLa genome, the Pu-Py mirror repeat tract elicits a polar replication fork barrier. Increased replication protein A (RPA), Rad9, and ataxia telangiectasia- and Rad3-related (ATR) checkpoint protein binding near the mirror repeat sequence suggests that the DNA damage response is activated upon replication fork stalling. Moreover, the proximal c-*myc* origin of replication was not required to cause orientation-dependent checkpoint activation. Cells expressing the replication fork barrier display constitutive Chk1 phosphorylation and continued growth, *i.e.* checkpoint adaptation. Excision of the Pu-Py mirror repeat tract abrogates the DNA damage response. Adaptation to Chk1 phosphorylation in cells expressing the replication fork barrier may allow the accumulation of mutations that would otherwise be remediated by the DNA damage response.

The polycystic kidney disease 1 (*PKD1*; Online Mendelian Inheritance in Man (OMIM) 173900) gene encodes the polycystin 1 protein, an integral membrane protein important for cell-cell adhesion and signal transduction (1). In humans, germline mutations in the *PKD1* gene (chromosome 16p) are associated with more than 85% of cases of autosomal dominant polycystic kidney disease. A screen for mutations in 131 unrelated patients with autosomal dominant polycystic kidney disease revealed that missense, polymorphism, and frameshift mutations were more than twice as frequent in exons 15–17 (1 per 49 bp) and 22–26 (1 per 48 bp), flanking intron 21 (IVS21), than in exons 1–8 (1 per 132 bp) (2), suggesting that the *PKD1* intron 21 may promote mutations in neighboring sequences.

The *PKD1* gene lies immediately adjacent to the tuberous sclerosis 2 (*TSC2*) tumor suppressor gene that is commonly mutated in tuberous sclerosis complex (3, 4). In a study of 45 unrelated tuberous sclerosis patients by Brook-Carter *et al.* (5), renal ultrasound revealed 18 patients with renal cysts. Of these patients, 11 also displayed renal angiomyolipomata (6), and six had severe infantile polycystic kidney disease with large chromosomal deletions disrupting both *TSC2* and *PKD1* (5, 7).

The *PKD1* locus contains a 2.5-kb polypurine-polypyrimidine (Pu-Py)[4] tract comprising several large mirror repeat sequences capable of forming triplex or G-quadruplex structures (8, 9). The *PKD1* Pu-Py sequences establish polar barriers to DNA replication (9) and form triplex structures visible by atomic force microscopy (10). Consistent with the view that an alternative DNA structure formed by the *PKD1* IVS21 is responsible for mutagenesis in polycystic kidney disease (11), Bacolla *et al.* (12) demonstrated that plasmids containing the *PKD1* IVS21 DNA sequence were recognized as DNA lesions by the nucleotide excision repair pathway and induced a DNA damage response in *Escherichia coli*, and Wang *et al.* (13) dem-

* This work was supported, in whole or in part, by National Institutes of Health Grants DK016458 (to J. J. B.) and GM53819 (to M. L.). This work was also supported by a grant from the WSU Boonshoft School of Medicine (to G. L.).
[1] To whom correspondence may be addressed. Tel.: 937-775-3125; Fax: 937-775-3730; E-mail: Guoqi.Liu@yahoo.com.
[2] Present address: Dept. of Chemistry and Applied Biological Sciences, South Dakota School of Mines and Technology, Rapid City, SD 57701.
[3] To whom correspondence may be addressed. Tel.: 937-775-3125; Fax: 937-775-3730; E-mail: Michael.Leffak@wright.edu.

[4] The abbreviations used are: Pu-Py, polypurine-polypyrimidine; FRT, FLP recombinase target; FLP, flip recombinase enzyme; DUE, DNA unwinding element; ATR, ataxia telangiectasia- and Rad3-related; RPA, replication protein A; qPCR, quantitative PCR; TF, triplex forward; TR, triplex reverse; DF, DUE forward; DR, DUE reverse; STS, sequence-tagged site(s).

onstrated that mutations are induced by triplex formation in SV40-derived plasmids replicating in COS-1 cells.

DNA sequences that are able to adopt non-B form alternative DNA structures represent obstructions to DNA replication and generate hotspots of chromosomal breakage, recombination, and rearrangement (14–17). In bacterial and yeast model systems, DNA hairpin-, triplex-, and G-quadruplex-forming sequences act as kinetic barriers to replication fork movement (18–24), which promote DNA double strand breaks (25, 26). Sequence alterations that increase the stability of alternative DNA structures *in vitro* also increase the mutability of these sequences *in vivo*, whereas knockdown of replication fork-stabilizing proteins or DNA damage sensors enhances the rate of mutation at alternative DNA structures (27–33). These observations implicate non-B forms of DNA generated during replication or repair in activating DNA damage checkpoints, promoting DNA breakage, and enhancing genome instability (34, 35).

DNA tracts that form alternative DNA structures are most often repetitive sequences. In the case of mirror repeat polypurine-polypyrimidine (Pu-Py) sequences, a DNA strand from one-half of the repeat can form a triple helix by folding back into the duplex major groove and pairing with a polypurine segment of the adjacent DNA through Hoogsteen or reverse Hoogsteen hydrogen bonding, whereas its complement remains single-stranded (10, 36). The polypurine strand of the *PKD1* IVS21 mirror repeat also contains multiple copies of the G-quadruplex consensus motif, most often at least four runs of three or more guanines. Therefore, Pu-Py sequences DNA could theoretically act to stall replication by sequestering template DNA in triplex or G-quadruplex structures (9, 20, 37) or, conversely, promote replication as origin DNA unwinding elements (38–40) by exposing single-stranded template to helicases or polymerases. Triplex structures have been detected *in vivo* (41), and the sequence-specific induction of mutation and recombination by triplex-forming oligonucleotides also suggests their *in vivo* existence (42). Indeed, instability at the FRDA locus in patients with Friedreich ataxia has been ascribed to triplex formation by GAA-TTC repeats that stall polymerases and promote chromosome recombination (43–45). Further evidence for *in vivo* effects of alternative DNA structures comes from model studies of the region between the P1 and P2 promoters of the human c-*myc* gene, which contains an asymmetric Pu-Py tract that can form triplex and G-quadruplex DNA (46). Mutations that destabilize the G-quadruplex enhanced c-*myc*-driven transcription in transient luciferase plasmid reporter assays (47), whereas mutations that enhanced triplex formation increased the frequency of mutation during plasmid replication assays (48).

In the present work, we show that the *PKD1* IVS21 88-bp Pu-Py mirror repeat sequence asymmetrically blocks primer extension *in vitro* and forms a polar barrier to plasmid DNA replication in cell extracts and human chromosome replication *in vivo*. To examine the effect of the IVS21 Pu-Py tract on human chromosomal DNA replication, the IVS21 Pu-Py sequence was cloned alongside the c-*myc* replication origin 2.4-kb core fragment and integrated at the single FLP recombinase target (FRT) site in the HeLa acceptor cell line 406 (49, 50). The c-*myc* core replicator integrated at this ectopic site displays the replication timing, chromatin structure, and replication protein (origin recognition complex (ORC), Cdc6, minichromosome maintenance (MCM), DUE-B, and Cdc45) binding of the endogenous c-*myc* origin (38, 51, 52). Clonal c-*myc*:Pu-Py cell lines were created in which the Py-rich sequence is replicated as the leading or lagging strand template from the neighboring c-*myc* origin to determine whether alternative DNA structure formation results in an orientation-dependent barrier to replication fork movement. Because triplex formation also results in an unpaired DNA strand (8), we also tested whether the Pu-Py sequence could act as a functional DNA unwinding element (DUE) for replication origin activity in clonal cell lines in which the *PKD1* Pu-Py mirror repeat sequence replaced the DUE of the c-*myc* replicator (39).

Using these cell lines, we demonstrate that the ectopic IVS21 sequence could not functionally replace the c-*myc* origin DUE, but was capable of orientation-dependent replication fork stalling when replicated from the proximal c-*myc* origin or from a distal chromosomal origin. When replicated from the neighboring c-*myc* origin, orientation-dependent fork stalling by the IVS21 Pu-Py sequence resulted in activation of the ataxia telangiectasia- and Rad3-related (ATR) and Chk1 DNA damage response pathway. Cells in which fork stalling occurred were able to adapt to this replication stress and continue cell division. FLP recombinase-mediated excision of the c-*myc*:Pu-Py cassette eliminated constitutive Chk1 phosphorylation. These results suggest that non-B DNA formed by the single copy IVS21 Pu-Py sequence directly and constitutively activates the cellular DNA damage response. In *PKD1* patients, adaptation may allow the accumulation of mutations that would otherwise be eliminated during cell cycle checkpoint arrest.

EXPERIMENTAL PROCEDURES

In Vitro Replication Extracts—Cytosolic extracts for *in vitro* DNA replication were prepared using $\sim 2 \times 10^8$ exponentially growing cells that were collected by centrifugation at $1000 \times g$, washed (at 5×10^6 cells/ml) with ice-cold isotonic buffer (20 mM Hepes, pH 7.5, 5 mM KCl, 1.5 mM $MgCl_2$, 1 mM dithiothreitol, and 250 mM sucrose), and again washed with the same volume of hypotonic buffer (isotonic buffer without sucrose) (53, 54). The cells were resuspended in hypotonic buffer, at $\sim 10^8$ cells/ml, and disrupted by Dounce homogenization. After incubation on ice for 45 min, cell extract supernatant was collected following centrifugation at $14{,}000 \times g$ for 10 min and stored in small aliquots at −70 °C.

Primer Extension Reactions—Reactions were performed essentially as described previously (9). The Pu-rich reaction template and primer were 5′-AGGGGGGAGGAGGGGAGGAGGGAGGAGGGGAGGAGGGGGGA-3′ and 5′-TCCCCCCTCCTCCCCTCCTC-3′, respectively; the Py-rich reaction template and primer were 5′-TCCCCCCTCCTCCCCTCCTCCCTCCTCCCCTCCTCCCCCCT-3′ and 5′-AGGGGGGAGGAGGGGAGGAG-3′, respectively; and the control reaction template and primer were 5′-AGGCATTTTGCTGCCGGTCAGGAGGAGGGGAGGAGGGGGGA-3′ and 5′-TCCCCCCTCCTCCCCTCCTC-3′ (same primer as in the Pu-rich template reaction), respectively.

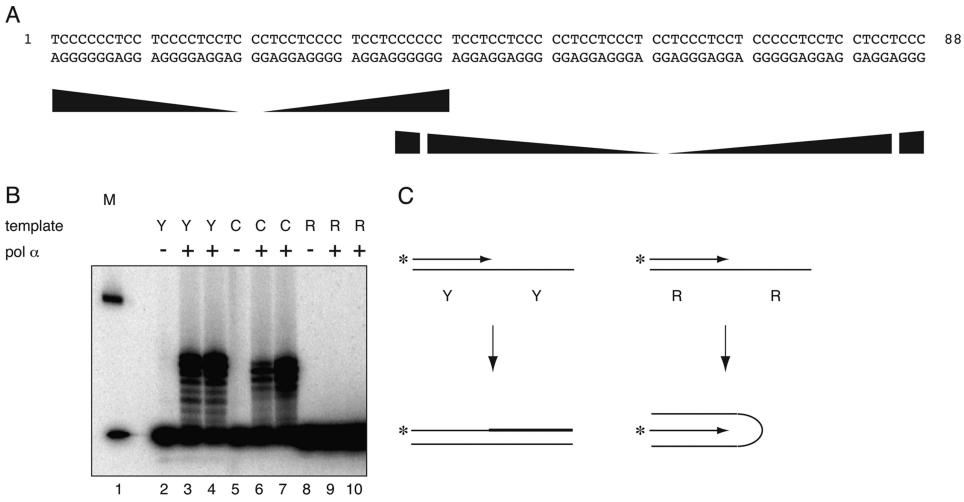

FIGURE 1. **The Pu-rich strand of the IVS21 88-bp mirror repeat Pu-Py sequence inhibits primer extension.** *A*, sequence of the 88-bp *PKD1* Pu-Py sequence. *Ramped shapes* indicate mirror symmetry repeats. *B*, primer extension. Bovine polymerase α (*pol α*) was used to extend primers on oligonucleotides containing the IVS21 Pu-rich (*R*) or Py-rich (*Y*) template sequence. At physiological pH, replication is inhibited only with the Pu-rich template. *Lane 1*, marker; *lanes 2*, *5*, and *8*, no polymerase; *lanes 3* and *4*, *6* and *7*, and *9* and *10*, contain the polypyrimidine (Py-rich) template, the control template (*C*), and the polypurine (Pu-rich) template at low and high polymerase concentration, respectively. *C*, interpretation of primer extension results.

In Vitro Replication—The 88-bp Pu-Py sequence from plasmid pJB4 (9) was cloned in pZ189 (5502 bp). Replication reactions (30 μl) contained 25 ng of plasmid template DNA; 100 μg of lymphoblast extract protein; 30 mM Hepes (pH 7.5); 100 μM each of dATP, dGTP, and dTTP; 50 μM dCTP; 10 μCi of [α-^{32}P]dCTP; 200 μM each of GTP, UTP, and CTP; 4 μM ATP; 40 mM creatine phosphate; 10 μg of creatine phosphokinase; and 1 μg of SV40 large T antigen (55, 56). Following incubation, reactions were terminated and purified by extraction with phenol and chloroform. Unincorporated radionucleotides were removed by spin dialysis against Tris-EDTA (pH 7.5), using a Centricon 30 microconcentrator. The reaction was extracted with phenol and chloroform and further digested by NdeI to release a fragment that was resolved using two-dimensional gel electrophoresis as described by Brewer and Fangman (57). The two dimensions were run under two different agarose concentrations such that length was resolved in the first dimension, and structure was resolved in the second (18, 57, 58).

Cell Culture—HeLa/406 acceptor cells containing a single chromosomal FLP recombinase target were constructed, grown, and transfected as described (49). FRT integrants were subjected to drug selection using G418 and ganciclovir (50). Cells were grown at 37 °C and 5% CO_2 in DMEM supplemented with 10% newborn calf serum. Nascent DNA was isolated from human cell lines by denaturing gel electrophoresis and quantitated by real time qPCR (38). qPCR results are based on at least two biological replicates (independent nascent DNA isolations) quantitated in triplicate. Cell lysates were prepared using M-Per reagent (Pierce). Chk1 was detected using antibody 2345, and phospho-Chk1$^{Ser\text{-}345}$ was detected using antibody 2341, both from Cell Signaling Technology.

ChIP—Immunoprecipitation of formaldehyde cross-linked chromatin was performed as described (52, 59). Antibodies used for chromatin immunoprecipitation were as follows: ATR (Santa Cruz Biotechnology sc-1887), RPA (Santa Cruz Biotechnology sc-25376), and Rad9 (Santa Cruz Biotechnology sc-8324).

Flow Cytometry—Cells were either untreated or treated with 2 μg/ml aphidicolin overnight or with UCN-01 (300 nM) (7-hydroxystaurosporine, a generous gift from Dr. Mirit Aladjem, National Institutes of Health) for the indicated times. The synchronized cells were then rinsed three times with PBS and refed with fresh drug-free medium. At the appropriate times, cells were trypsinized, washed with PBS, and fixed in cold 70% ethanol overnight. Cells were centrifuged at low speed and resuspended in PBS and then treated with 50 units/ml RNase A at 37 °C for 20 min. Propidium iodide (50 μg/ml) was added, and cells were incubated at 4 °C for 30 min. Cells were warmed to room temperature before processing.

Drug Treatment—After release from aphidicolin, cells were rinsed three times with PBS and fed with normal medium. Where indicated, medium was supplemented with 5 mM caffeine (Sigma) for 2 h.

RESULTS

Alternative DNA Structures Formed by the IVS21 Pu-Py Tract—At physiological pH, triplex or G-quadruplex formation occurs preferentially through the Pu-rich strand (60, 61), whereas acidic pH allows intramolecular triplex formation involving a protonated C-rich strand (62) in negatively supercoiled or relaxed DNA (8, 63). Bovine DNA polymerase α was used to assay for primer extension on the IVS21 mirror repeat (Fig. 1*A*) Py-rich strand or Pu-rich strand at physiological pH. As shown in Fig. 1*B*, the Pu-rich template did not allow primer extension, whereas a control template was efficiently extended using the same primer, as was the Py-rich template and its complementary primer, suggesting that the Pu-rich template strand adopts a conformation incompatible with DNA synthesis (Fig. 1*C*). These results are consistent with previous demonstrations that alternative DNA structure formation impedes bacterial DNA polymerases (20), although the current experiment does not allow unambiguous assignment of triplex or G-quadruplex structure to the Pu-rich IVS21 sequence because this template contains multiple matches to the G-quadruplex consensus

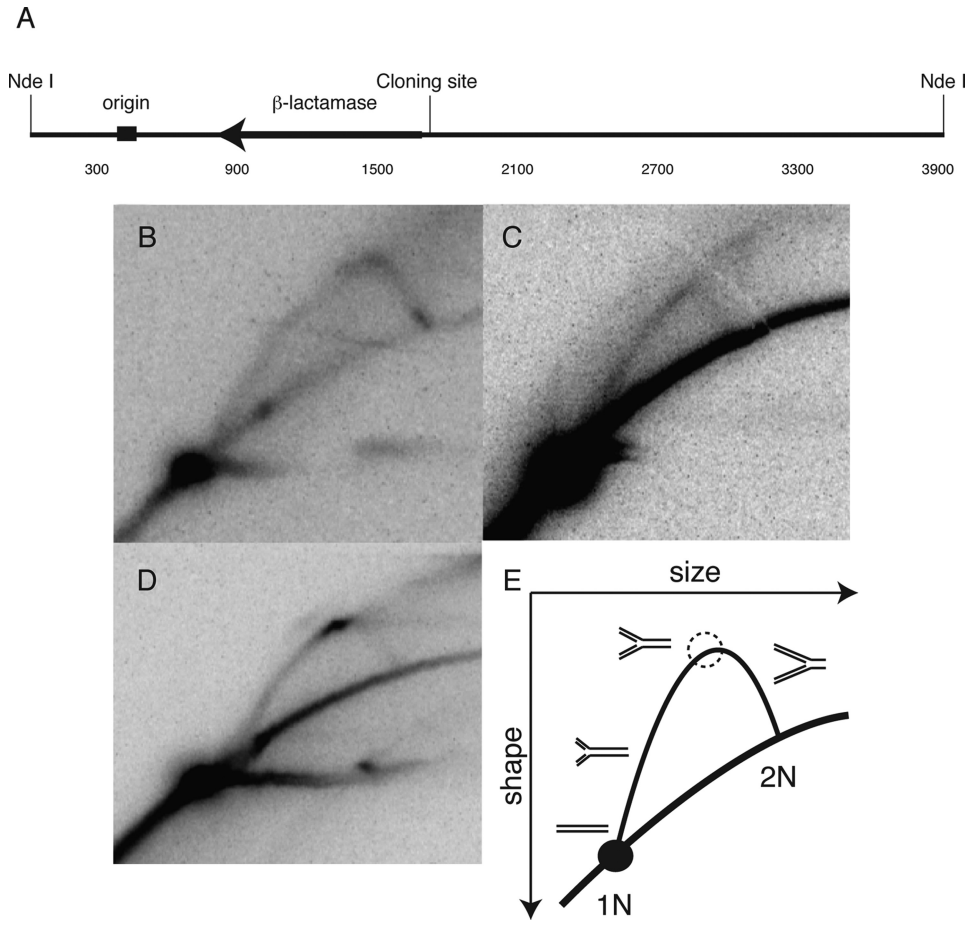

FIGURE 2. ***In vitro* replication demonstrates a polar replication blockade.** *A*, map of the SV40 origin of replication in relation to the cloning site of the *PKD1* mirror repeat sequences and the NdeI restriction endonuclease cut sites in the pZ189-based vector. *B*, neutral-neutral two-dimensional replication gel revealing a smooth Y arc of replication intermediates for the vector alone. *C*, a smooth Y-arc similar to the replication pattern of the vector alone is seen when leading strand synthesis encounters the Pu-rich template. *D*, a strong pause is seen when the Pu-rich sequence is in the lagging strand template. The horizontal signal extending from the 1N spot is commonly seen in plasmid replication (93). *E*, diagram explaining the results in *panel D*, depicting the increase in signal due to fork stalling (*dashed circle*, on arc of Y-intermediates).

(four runs of $G_{\geq 3}$, N_{0-6}), and either triplex and G-quadruplex formation is possible under these conditions.

The IVS21 Pu-Py Repeat Forms a Polar Replication Fork Barrier in Vitro—DNA sequences capable of forming noncanonical structures can stall replication forks in *vitro* and *in vivo* (9, 64). In the case of Pu-Py mirror repeat sequences, the orientation dependence of fork stalling suggests that inhibitory structures are formed when the Pu-rich strand becomes single-stranded. To test the effect of the IVS21 Pu-Py sequence on T antigen-dependent replication in human cell extracts, the *PKD1* 88-bp Pu-Py mirror repeat tract (*PKD1* nucleotides 34,575–34,662) was cloned downstream of the viral replication origin in the pZ189 SV40 shuttle vector such that the Pu-rich strand would be replicated as the leading strand template (forward orientation) or the lagging strand template (reverse orientation); replication intermediates were visualized by two-dimensional gel electrophoresis (18, 57, 58). The vector alone (Fig. 2*B*) or the vector with the IVS21 Pu-Py insert in the forward orientation (Fig. 2*C*) produced a smooth Y-arc. In contrast, the plasmid in which the Pu-rich strand was replicated as the lagging strand template showed a significant proportion of stalled replication forks, evident as a pronounced bulge in the Y-arc of replication intermediates (Fig. 2, *D* and *E*) (18, 23, 58, 65). Inasmuch as only the Pu-rich strand impedes *in vitro* replication at physiological pH (Fig. 1, *B* and *C*), these results imply that the Pu-rich strand forms a structure that inhibits replication fork progress when it is replicated as the lagging strand template. This contrasts with the replication polarity-independent stalling of replication forks at hairpin-forming $(CTG)_n$-$(CAG)_n$ trinucleotide repeats in replicating yeast plasmids (66, 67) and human chromosomal DNA (68).

Replication of the IVS21 Pu-Py Tract at an Ectopic Chromosomal Site in HeLa Cells—To determine the effect of the IVS21 Pu-Py 88-bp mirror repeat tract on replication in eucaryotic chromosomes, clonal c-*myc*:Pu-Py cell lines were constructed in which the mirror repeat Pu-Py tract was substituted for the c-*myc* replicator triplex-forming sequence (46) (TF and TR cells) and integrated at a unique ectopic FRT site (chromosome 18p11.22) (39, 49, 50, 67) (Fig. 3*A*). In the TF (triplex forward) cells, the Py-rich sequence is replicated as the lagging strand template from the neighboring c-*myc* origin, whereas in the TR (triplex reverse) cells, the Pu-rich sequence is replicated as the lagging strand template from the c-*myc* origin. We postulated that preferential triplex or G-quadruplex formation by foldback of the single-stranded Pu-rich lagging strand template in TR cells might result in an orientation-

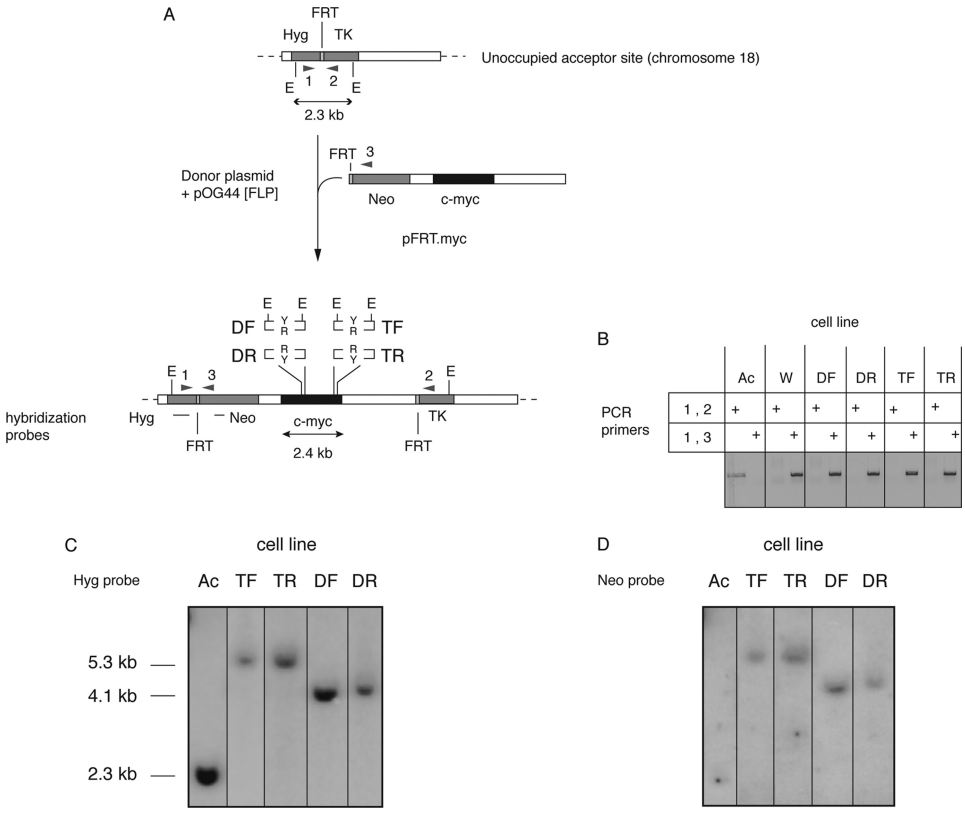

FIGURE 3. **Construction and validation of ectopic c-*myc*:Pu-Py cell lines.** *A*, a c-*myc* replicator construct containing the 88-bp IVS21 Pu-Py mirror repeat sequence was specifically integrated at the FRT (acceptor) site of the HeLa/406 acceptor cell line (94). Four constructs were used to create separate clonal cell lines. For TF or TR cell lines, the Pu-Py tract was inserted in place of the c-*myc* triplex-prone region in either the forward (Pu-rich strand replicated as the leading strand template) or the reverse (Pu-rich strand replicated as the lagging strand template) orientation, respectively. For DF and DR cell lines, the Pu-Py sequence was inserted in place of the c-*myc* DUE in the same orientations as in TF and TR cells, respectively. Sequence-tagged sites pBr and pML and hybridization probes Hyg and neomycin (*Neo*) are shown. *TK*, thymidine kinase. *B*, analytical PCR of acceptor and integrant cell line DNAs. A product with primer set *1,2* indicates an empty acceptor site, whereas a product with primer set *1,3* indicates integration of the c-*myc* construct. *Ac*, acceptor cell line (HeLa/406) without insert. *W*, acceptor cell line containing the wild type 2.4-kb c-*myc* core replicator. DF, DR, TF, and TR are c-*myc*:Pu-Py cell lines. *C* and *D*, Southern blot hybridization of genomic DNA from the indicated cell lines probed with Hyg (*C*) or neomycin (*Neo*) (*D*) probes. A single band of the correct size hybridizing to the Hyg probe demonstrates integration at the correct site. A single band of the correct size hybridizing to the neomycin probe indicates that only one copy of the insert had integrated into the genome.

dependent barrier to replication fork movement, as occurred during replication *in vitro*.

Under conditions of triplex formation, the 88-bp IVS21 sequence becomes sensitive to the P1 nuclease, reflecting the formation of single-stranded DNA (8). To assess whether the triplex-prone sequence could functionally substitute for the c-*myc* replicator DNA unwinding element (39, 50), a pair of cell lines, DF and DR, was engineered in which the IVS21 88-bp mirror repeat sequence was cloned in either orientation in place of the c-*myc* origin DUE (39) and integrated at the same chromosomal site. DF and DR cells contain the Py-rich sequence on the same DNA strands, respectively, as TF and TR cells.

Southern hybridization and PCR amplification confirmed that the c-*myc*:Pu-Py donor plasmids had integrated uniquely at the FRT (Fig. 3, *B–D*). To assess the replicator activity of the c-*myc* origin in these constructs, short (0.5–2.0-kb) nascent DNA from unsynchronized cells in logarithmic growth was quantitated by real time qPCR at two sites flanking the ectopic c-*myc* replicator (STS-pBR, -pML) and at a control distal site (STS-Hyg) (Fig. 4). As reported previously, deletion of the 201-bp c-*myc* DUE domain (ΔDUE) eliminated the origin activity of the wild type c-*myc* replicator (WT) (50), quantitated as relative nascent strand abundance, whereas previous work has shown that heterologous DUEs comprising expanded $(ATTCT)_{27}$ or $(ATTCT)_{48}$ pentanucleotide repeats from the *ATXN10/SCA10* locus could function as DUEs and restore ectopic origin activity (39). However, replacement of the c-*myc* DUE with the IVS21 Pu-Py repeat in either orientation did not restore origin activity to a level greater than that at an unoccupied FRT site or at the FRT site occupied by non-origin control sequences (49, 50). This indicates that although this sequence may have a greater tendency to form alternative DNA structures than nonrepetitive DNA, this tendency alone is not sufficient to replace the DUE functionality and restore origin activity.

In contrast, replacement of the c-*myc* triplex-forming sequence in TF and TR cells did not reduce origin activity when compared with cells containing the wild type c-*myc* origin, as evidenced by the similar nascent strand abundance at STS-pBR. However, a dramatic decrease of nascent strand abundance was observed downstream of the c-*myc* origin (at STS-pML) in TR cells, where the Pu-rich strand of the IVS21 repeat was replicated as the lagging strand template (Fig. 4*B*).

Orientation-dependent Replication Fork Stalling by the IVS21 Pu-Py Sequence—The nascent strand abundance upstream (STS-pBR) and downstream (STS-pML) of the ectopic c-*myc* origin activity of TF cells mirrors that of cells

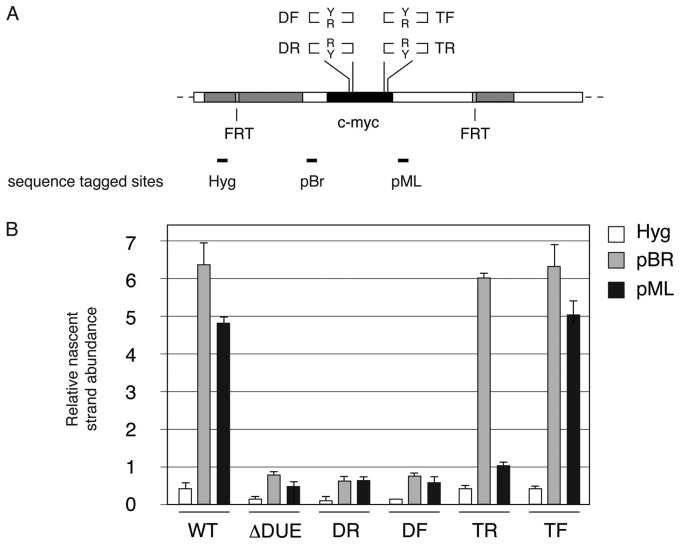

FIGURE 4. **Origin activity of c-*myc*:Pu-Py integrants.** *A*, diagram of the integration site in c-*myc*:Pu-Py cell lines DF, DR, TF, and TR, including sequence-tagged sites (STS) used for qPCR quantitation of nascent DNA. DF and DR contain the *PKD1* IVS21 88-bp mirror repeat sequence in place of the c-*myc* DUE; TF and TR contain the *PKD1* IVS21 88-bp mirror repeat sequence in place of the c-*myc* triplex-forming region. *R* and *Y* refer to the orientation of the Pu-rich and Py-rich strands of the 88-bp Pu-Py repeat, respectively. *B*, short, nascent DNA (0.5–2.0 kb) was harvested from the indicated cell lines and quantitated by qPCR at STS-Hyg, -pBR, and -pML. *WT*, wild type 2.4-kb c-*myc* core origin; Δ*DUE*, DUE deleted c-*myc* core origin. *Error bars* indicate S.D.

containing the wild type c-*myc* replicator (Fig. 4), suggesting that nascent strands initiating within the c-*myc* replicator progress bidirectionally without stalling when the Py-rich strand is replicated as the lagging strand template. In TR cells, however, there was a significant decrease in the quantity of short (0.5–2.0-kb) nascent DNA at STS-pML, suggesting that there is a barrier to nascent DNA synthesis between the origin and STS-pML when the Pu-rich strand is replicated as the lagging strand template. To confirm the asymmetry of nascent strand abundance in TR cells, one-step denaturing gel electrophoresis was used to size fractionate nascent DNA between 0.3 and 4.0 kb (39, 50).

When nascent DNA was isolated from c-*myc* WT, TF, or TR cells (Fig. 5*A*) and quantitated as shown in Fig. 5, *B* and *C*, the qPCR signal at STS-pBR was low in the 0.3–0.5- and 0.5–1.0-kb fractions and increased substantially in the 1.0–2.0- and 2.0–4.0-kb nascent DNAs, consistent with the distance between STS-pBR and the major initiation sites near the DUE of the c-*myc* replicator (69, 70). However, when quantitated at STS-pML, a reduction of ~4-fold was observed in 1.0–2.0- and 2.0–4.0-kb nascent DNA from TR cells when compared with WT c-*myc* or TF cells (Fig. 5*C*). The orientation dependence of the nascent strand depletion in TR cells argues that replication of the Pu-Py sequence in the orientation in which the Pu tract is replicated as the lagging strand template promotes the formation of a fork barrier that stalls the replicative polymerases *in vivo*.

DNA Damage Checkpoint Protein Binding near the Ectopic Pu-Py Sequence—The intra-S phase checkpoint response is activated when the MCM replicative helicase is dissociated from the replisome at barriers to DNA polymerization (71). Under these conditions, the ATR and Rad9-Rad1-Hus1 complex proteins are recruited to RPA-bound single-stranded DNA generated by fork opening in the absence of DNA synthesis (72–74). To investigate whether replication stalling by the IVS21 Pu-Py sequence correlated with checkpoint protein binding, cross-linked chromatin was immunoprecipitated with antibodies against the ATR, RPA70, or Rad9 proteins. In TR cells *versus* TF cells, each of these proteins was enriched near the downstream qPCR primer site pML proximal to the Pu-Py tract when compared with the occupancy at the upstream sequence-tagged site pBR (Fig. 5*D*). These results suggest that lagging strand replication of the Pu-rich template and polymerase stalling leads to activation of the ATR-Chk1 checkpoint signaling pathway. To test directly for activation of the ATR-Chk1 pathway in the four ectopic c-*myc*:Pu-Py cell lines (Fig. 6*A*), activated Chk1 (phosphorylated on serine 345, phospho-Chk1$^{Ser\text{-}345}$) was analyzed (75, 76). Phospho-Chk1$^{Ser\text{-}345}$ was not detected in TF cells (Fig. 6*B*). In contrast, phospho-Chk1$^{Ser\text{-}345}$ was observed constitutively in TR cells, and this phosphorylation was reduced by treatment of the cells with caffeine, an inhibitor of the ATR kinase (77).

Conversely, phospho-Chk1$^{Ser\text{-}345}$ was not detected in DR cells, but nominal caffeine-sensitive Chk1$^{Ser\text{-}345}$ phosphorylation was observed in DF cells (Fig. 6*C*). Because the c-*myc* replicator is inactive in DF and DR cells, the Pu-Py mirror repeat must be replicated from a neighboring origin, which previous work has estimated to be more than 4–8 kb downstream (49). The simplest explanation for the constitutive phosphorylation of Chk1$^{Ser\text{-}345}$ in DF cells but not DR cells is that the Pu-Py mirror repeat in the DF and DR cell populations is most often replicated from downstream origins, opposite to the direction of replication of the Pu-Py tract in TF and TR cells. In this scenario, the Pu-rich strand would be the lagging strand template in DF cells.

Phosphorylation of Chk1$^{Ser\text{-}345}$ was not observed in TF or DR cells. To confirm that TF and DR cells are capable of phosphorylating Chk1$^{Ser\text{-}345}$, the c-*myc*:Pu-Py cell lines were treated with the DNA polymerase inhibitor aphidicolin to activate the intra-S phase checkpoint (71). All four c-*myc*:Pu-Py cell lines responded to aphidicolin treatment by caffeine-sensitive phosphorylation of Chk1$^{Ser\text{-}345}$ (Fig. 6, *D* and *E*). However, the levels of phospho-Chk1$^{Ser\text{-}345}$ in TF and DR cells diminished within 3 h after removal of aphidicolin, whereas phospho-Chk1$^{Ser\text{-}345}$ remained at elevated levels in TR and DF cells following relief of the polymerase inhibition. Thus, the persistent phosphorylation of Chk1$^{Ser\text{-}345}$ in TR and DF cells but not in TF or DR cells suggests that the lagging strand replication of the IVS21 mirror repeat Pu-rich strand led to constitutive checkpoint activation during clonal expansion of the TR and DF cell lines. Surprisingly, only modest differences were detectable in the flow cytometry profiles of the four c-*myc*:Pu-Py cell lines (Fig. 6*F*). Taken together, these data imply that the presence of the Pu-rich mirror repeat in the lagging strand template orientation has caused constitutive Chk1$^{Ser\text{-}345}$ phosphorylation in TR and DF cells and that the continued proliferation of these cells reflects a process of checkpoint adaptation. Moreover, the rate of BrdUrd incorporation did not differ significantly between TF and TR cells, and these cells showed similar viability upon passage (data not shown).

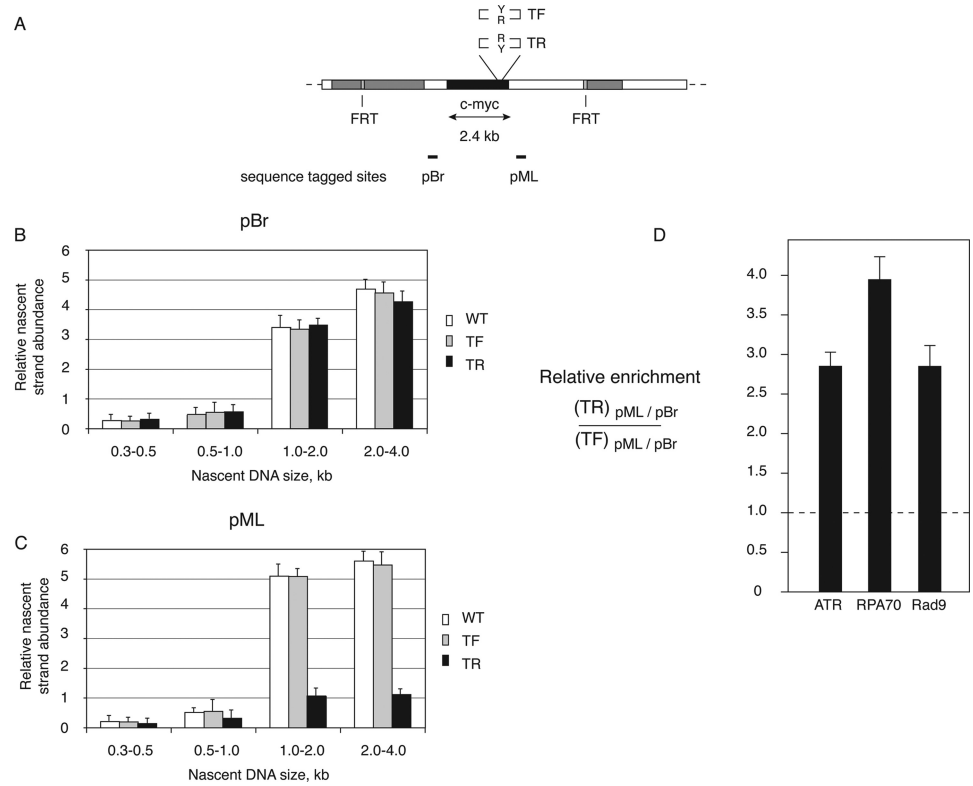

FIGURE 5. **The Pu-Py sequence forms a polar replication fork barrier in human cells.** Nascent DNA was isolated, size-fractionated, and analyzed by qPCR. *White bars*, cells containing ectopic wild type c-*myc* origin; *gray bars*, TF cells; *black bars*, TR cells. *A*, diagram of the integration site in c-*myc*:Pu-Py cell lines DF, DR, TF, and TR. *B*, nascent DNA abundance at STS-pBr. *C*, nascent DNA abundance at STS-pML. *D*, ATR, RPA, and Rad9 are enriched near the Pu-Py insert in TR cells. Chromatin immunoprecipitation was performed using antibodies for ATR, RPA70, or Rad9. Immunoprecipitated chromatin was quantitated by qPCR at STS-pBr and -pML. The ratio of signals from TR cell chromatin to TF cell chromatin at STS-pML was normalized to the signal at STS-pBR in the same immunoprecipitation. *Error bars* in *panels C–D* indicate S.D.

Excision of the Pu-Py Insert Restores a TF-like Phenotype to TR Cells—It is formally possible that the constitutive activation of the ATR-Chk1 pathway in TR is not due to the replication polarity of the Pu-Py repeat element from the c-*myc* origin, but to other genotypic differences that arose sporadically during clonal expansion of these cells. To test whether the single copy c-*myc*:Pu-Py tract was specifically responsible for Chk1$^{Ser\text{-}345}$ phosphorylation in TR cells, the ectopic c-*myc*:Pu-Py construct was excised from TR cells using FLP recombinase, and clonal lines from which the c-*myc*:Pu-Py tract had been removed were isolated by limiting dilution (referred to as FLP-TR1 and FLP-TR2 cells).

Excision of the ectopic c-*myc*:Pu-Py insert from FLP-TR1 and FLP-TR2 cells reversed the constitutive phosphorylation of Chk1$^{Ser\text{-}345}$ (Fig. 7, *A–D*). As in TR cells, aphidicolin treatment of FLP-TR1 and FLP-TR2 cells gave rise to prolonged caffeine-sensitive phosphorylation of Chk1$^{Ser\text{-}345}$. We further tested whether Chk1 kinase activity, and by extension the intra-S phase checkpoint, was important for the viability of TR and FLP-TR cells by treatment with the Chk1 kinase inhibitor UCN-01 (75, 78). As shown in Fig. 7*E*, TR cells showed a marked sensitivity to killing (appearance of sub-G_1 cells) by UCN-01. In contrast, FLP-TR1 and FLP-TR2 cells were resistant to killing by UCN-01 (Fig. 7*F*). We infer that additional mutations that may have accumulated during adaptation of the TR cells are not responsible for activation of the intra-S phase checkpoint and do not make the FLP-TR cells dependent on Chk1 kinase activity for survival.

DISCUSSION

The Pu-rich strand of the *PKD1* IVS21 mirror repeat forms a structure that is incompatible with primer extension *in vitro* and plasmid replication in human cell extracts. Considered with the orientation-dependent inhibition of replication by the Pu-Py mirror repeat tract in HeLa cells, our results suggest that non-B DNA structures formed during lagging strand replication of the Pu-rich template result in polymerase stalling and activation of the ATR-Chk1 checkpoint signaling pathway.

The distribution of mutations in the *PKD1* locus of patients with polycystic kidney disease implicates the IVS21 region as a focus of genomic instability (2). A mechanistic explanation for the instability posits that mirror repeat Pu-Py tracts in the IVS21 region hinder DNA polymerization and cause DNA double strand breaks, which are repaired by nonhomologous end joining (11). In support of this thesis, non-B DNA structures are known to inhibit replication fork progress (18, 20, 64) and activate DNA damage checkpoints (35, 79). Under physiological conditions, the Pu-rich strand may form G-quadruplex or triplex structures, whereas C-rich strand structures are less likely to occur *in vivo* as they are stabilized by hemiprotonated C-C$^+$ base pairing at acid pH (62, 80). Our results demonstrate that the *PKD1* IVS21 Pu-Py tract can inhibit primer extension on

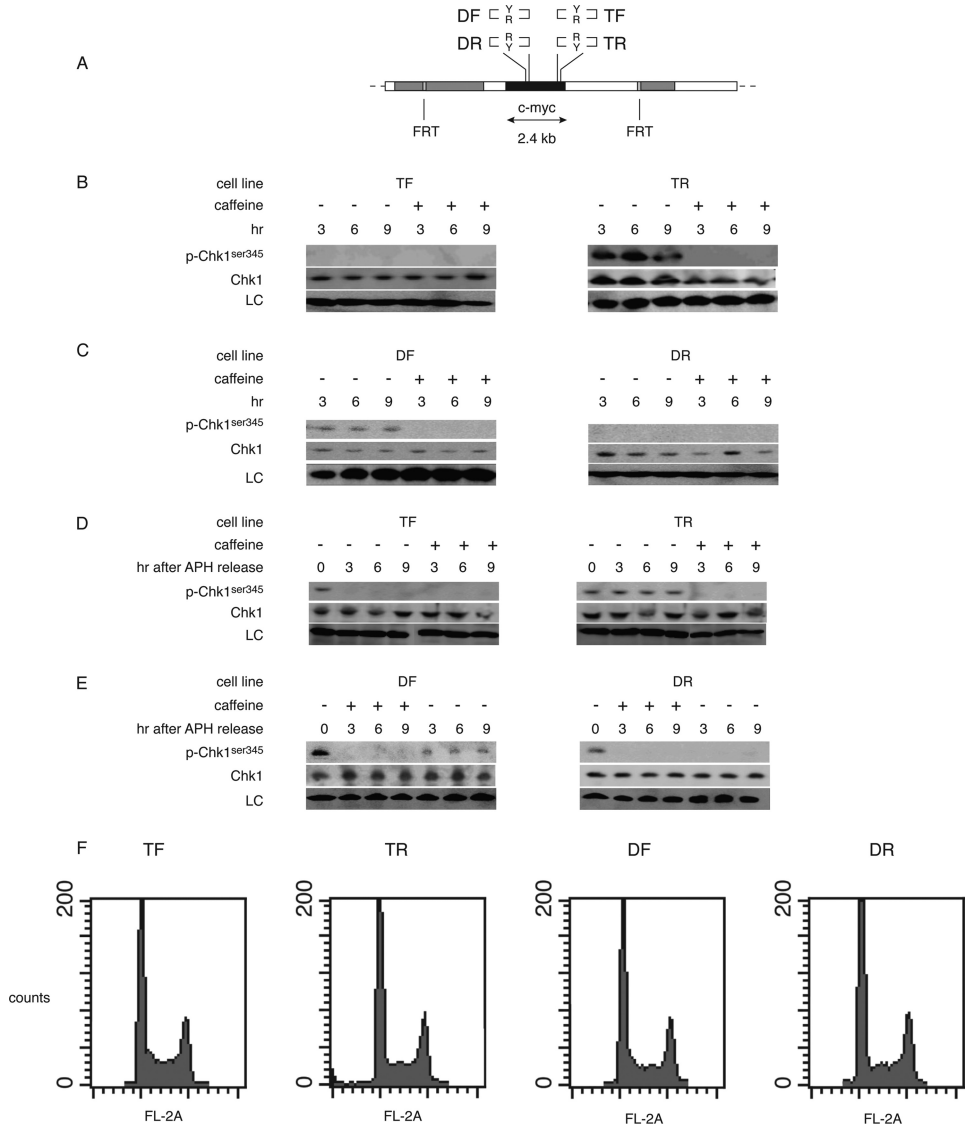

FIGURE 6. **Constitutive DNA damage response in TR and DF cells.** *A*, diagram of the integration site in c-*myc*:Pu-Py cell lines DF, DR, TF, and TR. *B* and *C*, whole cell extracts were isolated after treatment of cells with caffeine (+) for the indicated times (hours) or parallel untreated cultures (−) and immunoblotted for Chk1 and phospho-Chk1$^{Ser\text{-}345}$ (*p-Chk1^{ser345}*). *LC*, loading control. *D* and *E*, whole cell extracts were isolated after overnight treatment with aphidicolin and released into fresh control medium or medium containing caffeine for the indicated time and immunoblotted. *F*, flow cytometry profiles of asynchronous cultures of c-*myc*:Pu-Py cell lines.

purified DNA *in vitro* and in human chromosomes in a polar manner. Therefore, fork stalling is likely a consequence of an alternative structure of the Pu-Py mirror repeat DNA.

In TR cells, replication of the IVS21 Pu-rich strand as the lagging strand template results in fork stalling, checkpoint protein binding near the stalled fork, and activation of the Chk1 checkpoint kinase. The observation that TR and DF cells continue to divide at approximately the same rate as TF and DR cells suggests that the TR and DF cells have adapted to overcome cell cycle arrest (81, 82) despite constitutive Chk1 activation. Adaptation was originally described in *Saccharomyces cerevisiae* cells harboring a nonessential chromosome with an unrepaired HO endonuclease-induced double strand break, which could replicate the broken chromosome, proceed past the G_2/M checkpoint, and divide for several generations (82). Subsequent experiments using the same yeast strain showed that adaptation was defective in strains containing the *Cdc5-ad* Polo-like kinase mutant (81). In *Xenopus* egg extracts, nuclei could adapt to an aphidicolin-induced intra-S phase cell cycle checkpoint and proceed through mitosis. Adaptation involved Polo-like kinase Plx1 phosphorylation of Claspin, a replication fork-bound adaptor protein required for ATR activation of Chk1. Plx1 phosphorylation caused the release of Claspin from chromatin and the loss of Claspin-mediated Chk1 phosphorylation (83).

Down-regulation of Chk1 has also been implicated in checkpoint adaptation in human cells. Following ionizing radiation-induced G_2 checkpoint arrest, human U-2-OS osteosarcoma cells enter mitosis with γ-H2AX foci (76). Adaptation was promoted by inhibiting Chk1 and delayed by RNAi depletion of Plk1. The effects of Chk1 and Plk1 knockdown were additive; thus, the authors proposed that Chk1 and Plk1 may control the process of adaptation by independent signaling pathways. However, the exact mechanism of adaptation may differ in frog

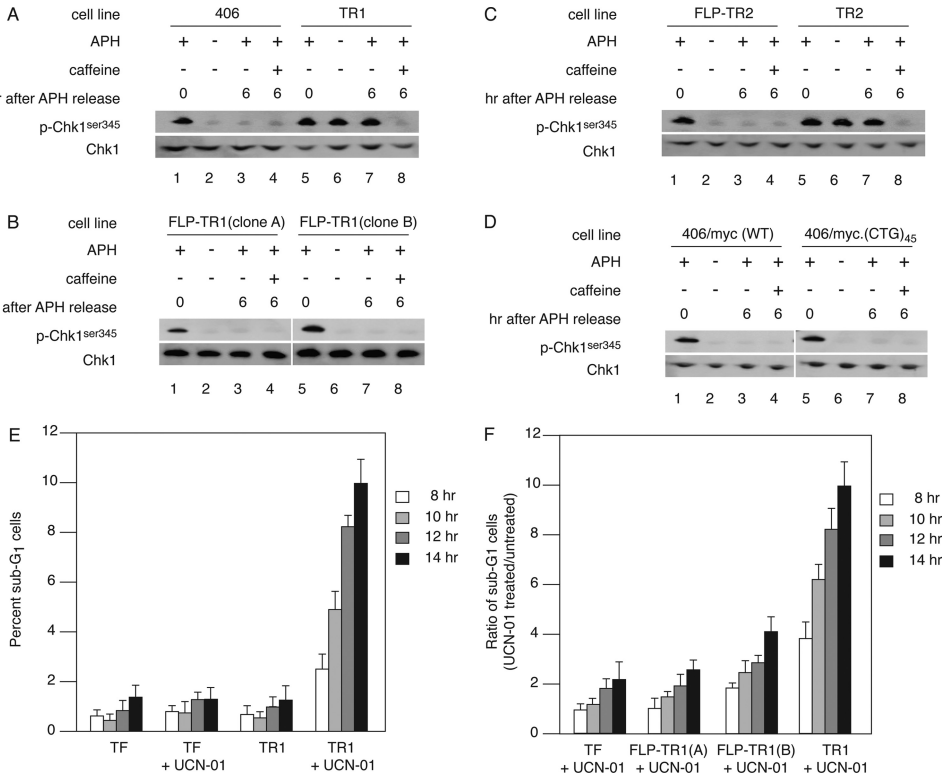

FIGURE 7. **Effects of excision of the c-*myc*:Pu-Py cassette.** *A*, Chk1 phosphorylation was compared in 406 acceptor cells and TR cells. *p-Chk1^{ser345}*, phospho-Chk1$^{Ser-345}$. *B*, TR1 cells were transfected with plasmid pOG44 encoding the *S. cerevisiae* FLP recombinase, and clonal cell lines from which the c-*myc*:Pu-Py cassette had been excised (*FLP-TR1(clone A)* and *FLP-TR1(clone B)*) were isolated by limiting dilution. Whole cell lysates were analyzed at the indicated times after aphidicolin treatment, without or with additional caffeine treatment, using anti-Chk1 or anti-phospho-Chk1$^{Ser-345}$ antibodies. *C*, the c-*myc*:Pu-Py cassette was excised by FLP recombinase from an independent line of TR cells (TR2), and Chk1 phosphorylation levels were compared. *D*, phospho-Chk1$^{Ser-345}$ are not elevated in cells containing the ectopic wild type c-*myc* replicator or the wild type c-*myc* replicator flanked by the $(CTG)_{45}$-$(CAG)_{45}$ hairpin-forming sequence (67). *E*, cells were synchronized with aphidicolin and released into normal medium or medium containing UCN-01 for 8, 10, 12, or 14 h before preparation for flow cytometry. The percentage of sub-G_1 cells in each sample at the release times indicated was plotted. Results are from four independent experiments. *F*, FLP-TR cells are less sensitive to UCN-01 treatment than TR cells. Cells were synchronized with aphidicolin and released into normal medium or medium containing UCN-01 for the indicated times. Plotted is the number of sub-G_1 cells in the sample released into UCN-01 divided by the number of sub-G_1 cells in a sister culture released into normal medium for the same amount of time. Data shown are representative of at least three experiments per cell line. *Error bars* in *panels E* and *F* indicate S.D.

egg extracts and humans because knockdown of Claspin did not accelerate mitotic entry of U-2-OS cells following ionizing radiation (76, 84).

In contrast to the foregoing models of adaptation, phospho-Chk1$^{Ser-345}$ levels remain elevated in dividing TR and DF cells. This raises the possibility that a checkpoint factor downstream of Chk1 has been altered in these cells. Because the HeLa cells used in the current experiments are deficient in p53 protein due to interaction with the HPV18 E6 protein (85), p53 and its transcriptional target, the cyclin-dependent kinase (CDK) inhibitor p21, are candidates. However, in HCT116 cells subjected to ionizing radiation, the initial G_2/M cell cycle arrest does not require p21 or p53, although these proteins are necessary to prolong the G_2/M arrest (86, 87). Likewise, HeLa cells retain the ability to arrest at the G_1/S phase and G_2/M phase cell cycle checkpoints (78, 87–89). Alternatively, the cellular reaction to high levels of DNA damage may differ from the responses to lower levels of damage encountered physiologically or the single genomic copy alternative DNA structures formed in TR and DF cells.

TR cells display elevated levels of phospho-Chk1$^{Ser-345}$ and are sensitive to killing by UCN-01 treatment, whereas FLP-TR cells do not display elevated levels of phospho-Chk1$^{Ser-345}$ and have decreased sensitivity to UCN-01. These observations suggest that constitutively activated Chk1 provides a function essential for viability that is specifically related to ameliorating the consequences of the activating lesion, *i.e.* the formation of a non-B DNA structure. One simple mechanism to accommodate these observations is that activated Chk1 stabilizes the replisome stalled by the non-B DNA structure and allows the Pu-Py sequence to be replicated in the opposite direction from a downstream replication origin.

Cell division with damaged DNA increases the risk of genome instability. In the context of *PKD1*, adaptation may lead to a mutator phenotype (90–92) and the subsequent accumulation of additional mutations (*e.g.* covalent DNA modification, expansion of repetitive DNA sequences, and mutations of genes encoding genome stabilization proteins). In this scenario, adaptation relies on the replication of the IVS21 Pu-Py mirror repeat as the lagging strand template in a subpopulation of kidney cells. Consistent with this suggestion, we have recently shown that the replication polarity of hairpin-forming sequences affects their pattern of instability in human cells (67). This model would suggest an evolutionary pressure for the selection of origin sites that minimize the formation of alternative DNA structures that stall replication.

REFERENCES

1. Wilson, P. D. (2001) Polycystin: new aspects of structure, function, and regulation. *J. Am. Soc. Nephrol.* **12,** 834–845
2. Rossetti, S., Strmecki, L., Gamble, V., Burton, S., Sneddon, V., Peral, B., Roy, S., Bakkaloglu, A., Komel, R., Winearls, C. G., and Harris, P. C. (2001) Mutation analysis of the entire *PKD1* gene: genetic and diagnostic implications. *Am. J. Hum. Genet.* **68,** 46–63
3. Green, A. J., Johnson, P. H., and Yates, J. R. (1994) The tuberous sclerosis gene on chromosome 9q34 acts as a growth suppressor. *Hum. Mol. Genet.* **3,** 1833–1834
4. Green, A. J., Smith, M., and Yates, J. R. (1994) Loss of heterozygosity on chromosome 16p13.3 in hamartomas from tuberous sclerosis patients. *Nat. Genet.* **6,** 193–196
5. Brook-Carter, P. T., Peral, B., Ward, C. J., Thompson, P., Hughes, J., Maheshwar, M. M., Nellist, M., Gamble, V., Harris, P. C., and Sampson, J. R. (1994) Deletion of the *TSC2* and *PKD1* genes associated with severe infantile polycystic kidney disease: a contiguous gene syndrome. *Nat. Genet.* **8,** 328–332
6. Bissler, J. J., and Kingswood, J. C. (2004) Renal angiomyolipomata. *Kidney Int.* **66,** 924–934
7. O'Callaghan, F. J., Noakes, M., and Osborne, J. P. (2000) Renal angiomyolipomata and learning difficulty in tuberous sclerosis complex. *J. Med. Genet.* **37,** 156–157
8. Blaszak, R. T., Potaman, V., Sinden, R. R., and Bissler, J. J. (1999) DNA structural transitions within the *PKD1* gene. *Nucleic Acids Res.* **27,** 2610–2617
9. Patel, H. P., Lu, L., Blaszak, R. T., and Bissler, J. J. (2004) *PKD1* intron 21: triplex DNA formation and effect on replication. *Nucleic Acids Res.* **32,** 1460–1468
10. Tiner, W. J., Sr., Potaman, V. N., Sinden, R. R., and Lyubchenko, Y. L. (2001) The structure of intramolecular triplex DNA: atomic force microscopy study. *J. Mol. Biol.* **314,** 353–357
11. Bissler, J. J. (2007) Triplex DNA and human disease. *Front. Biosci.* **12,** 4536–4546
12. Bacolla, A., Jaworski, A., Connors, T. D., and Wells, R. D. (2001) PKD1 unusual DNA conformations are recognized by nucleotide excision repair. *J. Biol. Chem.* **276,** 18597–18604
13. Wang, G., Seidman, M. M., and Glazer, P. M. (1996) Mutagenesis in mammalian cells induced by triple helix formation and transcription-coupled repair. *Science* **271,** 802–805
14. Sinden, R. R., and Wells, R. D. (1992) DNA structure, mutations, and human genetic disease. *Curr. Opin. Biotechnol.* **3,** 612–622
15. Bacolla, A., Wojciechowska, M., Kosmider, B., Larson, J. E., and Wells, R. D. (2006) The involvement of non-B DNA structures in gross chromosomal rearrangements. *DNA Repair* **5,** 1161–1170
16. Lobachev, K. S., Rattray, A., and Narayanan, V. (2007) Hairpin- and cruciform-mediated chromosome breakage: causes and consequences in eukaryotic cells. *Front. Biosci.* **12,** 4208–4220
17. Wang, G., and Vasquez, K. M. (2006) Non-B DNA structure-induced genetic instability. *Mutat. Res.* **598,** 103–119
18. Krasilnikova, M. M., and Mirkin, S. M. (2004) Replication stalling at Friedreich ataxia $(GAA)_n$ repeats *in vivo*. *Mol. Cell. Biol.* **24,** 2286–2295
19. Samadashwily, G. M., Raca, G., and Mirkin, S. M. (1997) Trinucleotide repeats affect DNA replication *in vivo*. *Nat. Genet.* **17,** 298–304
20. Krasilnikov, A. S., Panyutin, I. G., Samadashwily, G. M., Cox, R., Lazurkin, Y. S., and Mirkin, S. M. (1997) Mechanisms of triplex-caused polymerization arrest. *Nucleic Acids Res.* **25,** 1339–1346
21. Usdin, K., and Woodford, K. J. (1995) CGG repeats associated with DNA instability and chromosome fragility form structures that block DNA synthesis *in vitro*. *Nucleic Acids Res.* **23,** 4202–4209
22. Weaver, D. T., and DePamphilis, M. L. (1984) The role of palindromic and non-palindromic sequences in arresting DNA synthesis *in vitro* and *in vivo*. *J. Mol. Biol.* **180,** 961–986
23. Voineagu, I., Narayanan, V., Lobachev, K. S., and Mirkin, S. M. (2008) Replication stalling at unstable inverted repeats: interplay between DNA hairpins and fork stabilizing proteins. *Proc. Natl. Acad. Sci. U.S.A.* **105,** 9936–9941
24. Rao, B. S. (1996) Regulation of DNA replication by homopurine/homopyrimidine sequences. *Mol. Cell. Biochem.* **156,** 163–168
25. Michel, B., Ehrlich, S. D., and Uzest, M. (1997) DNA double strand breaks caused by replication arrest. *EMBO J.* **16,** 430–438
26. Lambert, S., Watson, A., Sheedy, D. M., Martin, B., and Carr, A. M. (2005) Gross chromosomal rearrangements and elevated recombination at an inducible site-specific replication fork barrier. *Cell* **121,** 689–702
27. Freudenreich, C. H., Kantrow, S. M., and Zakian, V. A. (1998) Expansion and length-dependent fragility of CTG repeats in yeast. *Science* **279,** 853–856
28. Schweitzer, J. K., and Livingston, D. M. (1998) Expansions of CAG repeat tracts are frequent in a yeast mutant defective in Okazaki fragment maturation. *Hum. Mol. Genet.* **7,** 69–74
29. Callahan, J. L., Andrews, K. J., Zakian, V. A., and Freudenreich, C. H. (2003) Mutations in yeast replication proteins that increase CAG/CTG expansions also increase repeat fragility. *Mol. Cell. Biol.* **23,** 7849–7860
30. Lahiri, M., Gustafson, T. L., Majors, E. R., and Freudenreich, C. H. (2004) Expanded CAG repeats activate the DNA damage checkpoint pathway. *Mol. Cell* **15,** 287–293
31. Entezam, A., and Usdin, K. (2008) ATR protects the genome against CGG-CCG repeat expansion in Fragile X premutation mice. *Nucleic Acids Res.* **36,** 1050–1056
32. Voineagu, I., Freudenreich, C. H., and Mirkin, S. M. (2009) Checkpoint responses to unusual structures formed by DNA repeats. *Mol. Carcinog.* **48,** 309–318
33. Razidlo, D. F., and Lahue, R. S. (2008) Mrc1, Tof1, and Csm3 inhibit CAG-CTG repeat instability by at least two mechanisms. *DNA Repair* **7,** 633–640
34. Branzei, D., and Foiani, M. (2009) The checkpoint response to replication stress. *DNA Repair* **8,** 1038–1046
35. Lambert, S., Froget, B., and Carr, A. M. (2007) Arrested replication fork processing: interplay between checkpoints and recombination. *DNA Repair* **6,** 1042–1061
36. Frank-Kamenetskii, M. D., and Mirkin, S. M. (1995) Triplex DNA structures. *Annu. Rev. Biochem.* **64,** 65–95
37. Kang, S., Ohshima, K., Shimizu, M., Amirhaeri, S., and Wells, R. D. (1995) Pausing of DNA synthesis *in vitro* at specific loci in CTG and CGG triplet repeats from human hereditary disease genes. *J. Biol. Chem.* **270,** 27014–27021
38. Chowdhury, A., Liu, G., Kemp, M., Chen, X., Katrangi, N., Myers, S., Ghosh, M., Yao, J., Gao, Y., Bubulya, P., and Leffak, M. (2010) The DNA unwinding element-binding protein DUE-B interacts with Cdc45 in preinitiation complex formation. *Mol. Cell. Biol.* **30,** 1495–1507
39. Liu, G., Bissler, J. J., Sinden, R. R., and Leffak, M. (2007) Unstable spinocerebellar ataxia type 10 (ATTCT)-(AGAAT) repeats are associated with aberrant replication at the ATX10 locus and replication origin-dependent expansion at an ectopic site in human cells. *Mol. Cell. Biol.* **27,** 7828–7838
40. Kemp, M., Bae, B., Yu, J. P., Ghosh, M., Leffak, M., and Nair, S. K. (2007) Structure and function of the c-*myc* DNA-unwinding element-binding protein DUE-B. *J. Biol. Chem.* **282,** 10441–10448
41. Ussery, D. W., and Sinden, R. R. (1993) Environmental influences on the *in vivo* level of intramolecular triplex DNA in *Escherichia coli*. *Biochemistry* **32,** 6206–6213
42. Faruqi, A. F., Datta, H. J., Carroll, D., Seidman, M. M., and Glazer, P. M. (2000) Triple-helix formation induces recombination in mammalian cells via a nucleotide excision repair-dependent pathway. *Mol. Cell. Biol.* **20,** 990–1000
43. Wells, R. D. (2008) DNA triplexes and Friedreich ataxia. *FASEB J.* **22,** 1625–1634
44. Usdin, K., and Grabczyk, E. (2000) DNA repeat expansions and human disease. *Cell. Mol. Life Sci.* **57,** 914–931
45. Grabczyk, E., and Usdin, K. (2000) The GAA-TTC triplet repeat expanded in Friedreich ataxia impedes transcription elongation by T7 RNA polymerase in a length and supercoil dependent manner. *Nucleic Acids Res.* **28,** 2815–2822
46. Belotserkovskii, B. P., De Silva, E., Tornaletti, S., Wang, G., Vasquez, K. M., and Hanawalt, P. C. (2007) A triplex-forming sequence from the human c-*MYC* promoter interferes with DNA transcription. *J. Biol. Chem.* **282,**

32433–32441
47. Siddiqui-Jain, A., Grand, C. L., Bearss, D. J., and Hurley, L. H. (2002) Direct evidence for a G-quadruplex in a promoter region and its targeting with a small molecule to repress c-*MYC* transcription. *Proc. Natl. Acad. Sci. U.S.A.* **99,** 11593–11598
48. Wang, G., and Vasquez, K. M. (2004) Naturally occurring H-DNA-forming sequences are mutagenic in mammalian cells. *Proc. Natl. Acad. Sci. U.S.A.* **101,** 13448–13453
49. Malott, M., and Leffak, M. (1999) Activity of the c-*myc* replicator at an ectopic chromosomal location. *Mol. Cell. Biol.* **19,** 5685–5695
50. Liu, G., Malott, M., and Leffak, M. (2003) Multiple functional elements comprise a mammalian chromosomal replicator. *Mol. Cell. Biol.* **23,** 1832–1842
51. Kemp, M. G., Ghosh, M., Liu, G., and Leffak, M. (2005) The histone deacetylase inhibitor trichostatin A alters the pattern of DNA replication origin activity in human cells. *Nucleic Acids Res.* **33,** 325–336
52. Ghosh, M., Kemp, M., Liu, G., Ritzi, M., Schepers, A., and Leffak, M. (2006) Differential binding of replication proteins across the human c-*myc* replicator. *Mol. Cell. Biol.* **26,** 5270–5283
53. Li, J. J., and Kelly, T. J. (1985) Simian virus 40 DNA replication *in vitro*: specificity of initiation and evidence for bidirectional replication. *Mol. Cell. Biol.* **5,** 1238–1246
54. Li, J. J., and Kelly, T. J. (1984) Simian virus 40 DNA replication *in vitro*. *Proc. Natl. Acad. Sci. U.S.A.* **81,** 6973–6977
55. Carty, M. P., Hauser, J., Levine, A. S., and Dixon, K. (1993) Replication and mutagenesis of UV-damaged DNA templates in human and monkey cell extracts. *Mol. Cell. Biol.* **13,** 533–542
56. Carty, M. P., Lawrence, C. W., and Dixon, K. (1996) Complete replication of plasmid DNA containing a single UV-induced lesion in human cell extracts. *J. Biol. Chem.* **271,** 9637–9647
57. Brewer, B. J., and Fangman, W. L. (1987) The localization of replication origins on ARS plasmids in *S. cerevisiae*. *Cell* **51,** 463–471
58. Krasilnikova, M. M., and Mirkin, S. M. (2004) Analysis of triplet repeat replication by two-dimensional gel electrophoresis. *Methods Mol. Biol.* **277,** 19–28
59. Ghosh, M., Liu, G., Randall, G., Bevington, J., and Leffak, M. (2004) Transcription factor binding and induced transcription alter chromosomal c-*myc* replicator activity. *Mol. Cell. Biol.* **24,** 10193–10207
60. Plum, G. E., Park, Y. W., Singleton, S. F., Dervan, P. B., and Breslauer, K. J. (1990) Thermodynamic characterization of the stability and the melting behavior of a DNA triplex: a spectroscopic and calorimetric study. *Proc. Natl. Acad. Sci. U.S.A.* **87,** 9436–9440
61. Inoue, M., Miyoshi, D., and Sugimoto, N. (2005) Structural switch of telomere DNA by pH and monovalent cation. *Nucleic Acids Symp. Ser.* (*Oxf.*) 243–244
62. Kendrick, S., Akiyama, Y., Hecht, S. M., and Hurley, L. H. (2009) The i-motif in the bcl-2 P1 promoter forms an unexpectedly stable structure with a unique 8:5:7 loop folding pattern. *J. Am. Chem. Soc.* **131,** 17667–17676
63. Htun, H., and Dahlberg, J. E. (1989) Topology and formation of triple-stranded H-DNA. *Science* **243,** 1571–1576
64. Mirkin, E. V., and Mirkin, S. M. (2007) Replication fork stalling at natural impediments. *Microbiol. Mol. Biol. Rev.* **71,** 13–35
65. Voineagu, I., Surka, C. F., Shishkin, A. A., Krasilnikova, M. M., and Mirkin, S. M. (2009) Replisome stalling and stabilization at CGG repeats, which are responsible for chromosomal fragility. *Nat. Struct. Mol. Biol.* **16,** 226–228
66. Pelletier, R., Krasilnikova, M. M., Samadashwily, G. M., Lahue, R., and Mirkin, S. M. (2003) Replication and expansion of trinucleotide repeats in yeast. *Mol. Cell. Biol.* **23,** 1349–1357
67. Liu, G., Chen, X., Bissler, J. J., Sinden, R. R., and Leffak, M. (2010) Replication-dependent instability at (CTG)-(CAG) repeat hairpins in human cells. *Nat. Chem. Biol.* **6,** 652–659
68. Liu, G., Chen, X., Gao, Y., Lewis, T., Barthelemy, J., and Leffak, M. (2012) Altered replication in human cells promotes DMPK $(CTG)_n$-$(CAG)_n$ repeat instability. *Mol. Cell. Biol.* **32,** 1618–1632
69. Trivedi, A., Waltz, S. E., Kamath, S., and Leffak, M. (1998) Multiple initiations in the c-*myc* replication origin independent of chromosomal location. *DNA Cell Biol.* **17,** 885–896
70. Berberich, S., Trivedi, A., Daniel, D. C., Johnson, E. M., and Leffak, M. (1995) *In vitro* replication of plasmids containing human c-*myc* DNA. *J. Mol. Biol.* **245,** 92–109
71. Byun, T. S., Pacek, M., Yee, M. C., Walter, J. C., and Cimprich, K. A. (2005) Functional uncoupling of MCM helicase and DNA polymerase activities activates the ATR-dependent checkpoint. *Genes Dev.* **19,** 1040–1052
72. Choi, J. H., Lindsey-Boltz, L. A., Kemp, M., Mason, A. C., Wold, M. S., and Sancar, A. (2010) Reconstitution of RPA-covered single-stranded DNA-activated ATR-Chk1 signaling. *Proc. Natl. Acad. Sci. U.S.A.* **107,** 13660–13665
73. Yan, S., and Michael, W. M. (2009) TopBP1 and DNA polymerase α-mediated recruitment of the 9-1-1 complex to stalled replication forks: implications for a replication restart-based mechanism for ATR checkpoint activation. *Cell Cycle* **8,** 2877–2884
74. Xu, Y. J., and Leffak, M. (2010) ATRIP from TopBP1 to ATR: *in vitro* activation of a DNA damage checkpoint. *Proc. Natl. Acad. Sci. U.S.A.* **107,** 13561–13562
75. Zhao, H., and Piwnica-Worms, H. (2001) ATR-mediated checkpoint pathways regulate phosphorylation and activation of human Chk1. *Mol. Cell. Biol.* **21,** 4129–4139
76. Syljuåsen, R. G., Jensen, S., Bartek, J., and Lukas, J. (2006) Adaptation to the ionizing radiation-induced G_2 checkpoint occurs in human cells and depends on checkpoint kinase 1 and Polo-like kinase 1 kinases. *Cancer Res.* **66,** 10253–10257
77. Rodríguez-Bravo, V., Guaita-Esteruelas, S., Florensa, R., Bachs, O., and Agell, N. (2006) Chk1- and Claspin-dependent but ATR/ATM- and Rad17-independent DNA replication checkpoint response in HeLa cells. *Cancer Res.* **66,** 8672–8679
78. Jackson, J. R., Gilmartin, A., Imburgia, C., Winkler, J. D., Marshall, L. A., and Roshak, A. (2000) An indolocarbazole inhibitor of human checkpoint kinase (Chk1) abrogates cell cycle arrest caused by DNA damage. *Cancer Res.* **60,** 566–572
79. Lambert, S., and Carr, A. M. (2005) Checkpoint responses to replication fork barriers. *Biochimie* **87,** 591–602
80. Bucek, P., Jaumot, J., Aviñó, A., Eritja, R., and Gargallo, R. (2009) pH-modulated Watson-Crick duplex-quadruplex equilibria of guanine-rich and cytosine-rich DNA sequences 140 bp upstream of the c-*kit* transcription initiation site. *Chemistry* **15,** 12663–12671
81. Toczyski, D. P., Galgoczy, D. J., and Hartwell, L. H. (1997) CDC5 and CKII control adaptation to the yeast DNA damage checkpoint. *Cell* **90,** 1097–1106
82. Sandell, L. L., and Zakian, V. A. (1993) Loss of a yeast telomere: arrest, recovery, and chromosome loss. *Cell* **75,** 729–739
83. Yoo, H. Y., Kumagai, A., Shevchenko, A., Shevchenko, A., and Dunphy, W. G. (2004) Adaptation of a DNA replication checkpoint response depends upon inactivation of Claspin by the Polo-like kinase. *Cell* **117,** 575–588
84. Syljuåsen, R. G. (2007) Checkpoint adaptation in human cells. *Oncogene* **26,** 5833–5839
85. Scheffner, M., Werness, B. A., Huibregtse, J. M., Levine, A. J., and Howley, P. M. (1990) The E6 oncoprotein encoded by human papillomavirus types 16 and 18 promotes the degradation of p53. *Cell* **63,** 1129–1136
86. Bunz, F., Dutriaux, A., Lengauer, C., Waldman, T., Zhou, S., Brown, J. P., Sedivy, J. M., Kinzler, K. W., and Vogelstein, B. (1998) Requirement for p53 and p21 to sustain G_2 arrest after DNA damage. *Science* **282,** 1497–1501
87. Koniaras, K., Cuddihy, A. R., Christopoulos, H., Hogg, A., and O'Connell, M. J. (2001) Inhibition of Chk1-dependent G_2 DNA damage checkpoint radiosensitizes p53 mutant human cells. *Oncogene* **20,** 7453–7463
88. Karnani, N., and Dutta, A. (2011) The effect of the intra-S-phase checkpoint on origins of replication in human cells. *Genes Dev.* **25,** 621–633
89. Collis, S. J., Barber, L. J., Clark, A. J., Martin, J. S., Ward, J. D., and Boulton, S. J. (2007) HCLK2 is essential for the mammalian S-phase checkpoint and impacts on Chk1 stability. *Nat. Cell Biol.* **9,** 391–401
90. Kai, M., and Wang, T. S. (2003) Checkpoint responses to replication stalling: inducing tolerance and preventing mutagenesis. *Mutat. Res.* **532,** 59–73

91. Loeb, L. A., Loeb, K. R., and Anderson, J. P. (2003) Multiple mutations and cancer. *Proc. Natl. Acad. Sci. U.S.A.* **100,** 776–781
92. Prindle, M. J., Fox, E. J., and Loeb, L. A. (2010) The mutator phenotype in cancer: molecular mechanisms and targeting strategies. *Curr. Drug Targets* **11,** 1296–1303
93. Schvartzman, J. B., Martínez-Robles, M. L., Hernández, P., and Krimer, D. B. (2010) Plasmid DNA replication and topology as visualized by two-dimensional agarose gel electrophoresis. *Plasmid* **63,** 1–10
94. Liu, P., Barkley, L. R., Day, T., Bi, X., Slater, D. M., Alexandrow, M. G., Nasheuer, H. P., and Vaziri, C. (2006) The Chk1-mediated S-phase checkpoint targets initiation factor Cdc45 via a Cdc25A/Cdk2-independent mechanism. *J. Biol. Chem.* **281,** 30631–30644